

Short Note

# N-(4-Methyl-3-((4-(pyridin-3-yl)pyrimidin-2-yl)amino)phenyl)-4-((4-methylpiperazin-1-yl)methyl)benzamide

Alexander A. Korlyukov <sup>1</sup>, Pavel V. Dorovatovskii <sup>2</sup> and Anna V. Vologzhanina <sup>1,\*</sup>

<sup>1</sup> A. N. Nesmeyanov Institute of Organoelement Compounds, Russian Academy of Sciences, 28 Vavilov St., Moscow 119334, Russia

<sup>2</sup> National Research Center “Kurchatov Institute”, 1 Kurchatova pl., Moscow 123098, Russia

\* Correspondence: vologzhanina@mail.ru

**Abstract:** *Imatinib* is one of the most used therapeutic agents to treat leukemia, which specifically inhibits the activity of tyrosine kinases. This polytopic molecule has been structurally characterized only in the form of its piperazin-1-ium salt (mesylate, picrate, citrate, fumarate or malonate). Herein we present the crystal structure of the freebase *Imatinib* which precipitated from a 1:10 mixture with arginine. The molecule realizes an extended conformation and forms infinite H-bonded chains through its amide, amine and pyrimidine groups.

**Keywords:** active pharmaceutical ingredient; H-bond propensity; *Imatinib*; single-crystal X-ray diffraction



**Citation:** Korlyukov, A.A.; Dorovatovskii, P.V.; Vologzhanina, A.V. N-(4-Methyl-3-((4-(pyridin-3-yl)pyrimidin-2-yl)amino)phenyl)-4-((4-methylpiperazin-1-yl)methyl)benzamide. *Molbank* **2022**, *2022*, M1461. <https://doi.org/10.3390/M1461>

Academic Editor: Rodrigo Abonia

Received: 21 September 2022

Accepted: 7 October 2022

Published: 9 October 2022

**Publisher's Note:** MDPI stays neutral with regard to jurisdictional claims in published maps and institutional affiliations.



**Copyright:** © 2022 by the authors. Licensee MDPI, Basel, Switzerland. This article is an open access article distributed under the terms and conditions of the Creative Commons Attribution (CC BY) license (<https://creativecommons.org/licenses/by/4.0/>).

## 1. Introduction

*Imatinib* commercially available as Gleevec (Figure 1a) is the first therapeutic agent to treat chronic myelogenic leukemia [1,2]. A series of structural studies elucidated that *Imatinib* specifically binds to an inactive Abelson tyrosine kinase domain characteristic for this gene through numerous hydrogen bonds, hydrophobic C–H ...  $\pi$  and  $\pi$  ...  $\pi$  interactions [3,4]. Golzarroshan et al. compared its conformations in single crystals and ligand–protein complexes, and revealed that this flexible molecule realizes in crystals two main conformations, an extended with the pyridylpyrimidine moiety in trans position towards the methylbenzene ring and a folded with the pyridylpyrimidine moiety cis situated to the methylbenzene ring [5]. Analysis of contributions of various types of intermolecular interactions to the molecular surface revealed that  $\pi$  ...  $\pi$  stacking is more typical for the folded conformation of *Imatinib* [6], while the contribution of hydrophilic interactions does not affect molecular conformation.

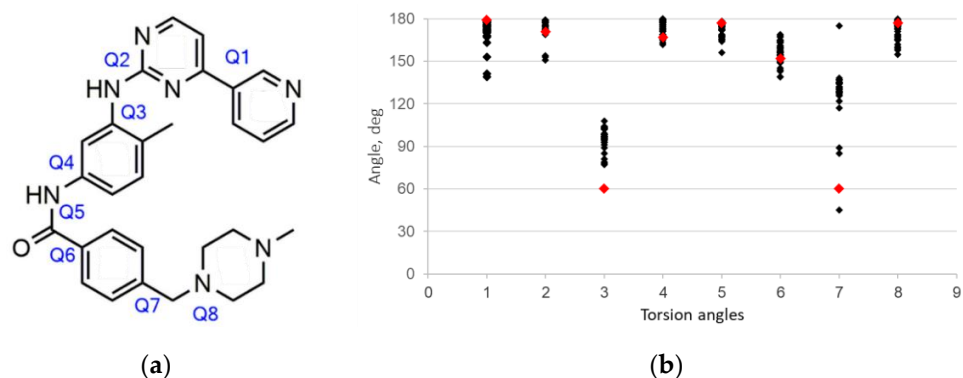


**Figure 1.** (a) Schematic representation of a freebase *Imatinib*. Q1–Q8 denote torsion angles. (b) Modules of Q1–Q8 angles of *Imatinib* in previously reported (black) and freebase (red) compounds in the extended conformation.

Both in crystals, and in ligand–receptor complexes *Imatinib* is present in the form of a mono- or a dication. Its commercial form contains *Imatinib* mesylate which exists in two polymorph modifications [7]. Besides mesylate, it readily forms salts with picrate [5,8], citrate [9], fumarate [9] or malonate [9] anions. Hybrid materials of *Imatinib* with nanodispersed MoS<sub>2</sub> sheets were obtained as well [10]. However, the crystal structure of the neutral freebase remained unknown to date, although its powder XRD solution was mentioned recently by Kabova et al. [11]. In this report we present the characterization of freebase *Imatinib* using single crystal X-ray diffraction.

## 2. Results and Discussion

In our study of novel solid forms of known active pharmaceutical ingredients [12], the potential of *Imatinib* to co-crystallize with amino acids was attested. A solution of *Imatinib* mesylate in ethanol was added to a solution of alanine, arginine, asparagine, glycine, isoleucine, methionine, tyrosine, serine or valine in ethanol in 1:10 molar ratio. A few drops of HNO<sub>3</sub> or heating were applied to make the solution transparent. After several days of standing in air at r.t., white precipitate formed in all cases. Typically, precipitate contained initial reagents; however, from *Imatinib*: arginine mixture, single crystals of the freebase *Imatinib* were obtained suitable for X-ray diffraction using synchrotron radiation.

The molecular structure of the freebase is represented on Figure 2. All hydrogen atoms were visible on difference Fourier maps; thus, one can conclude from both bond distances and residual density maps that only N4 amine and N5 amide nitrogen atoms are protonated. The values Q1–Q8 of torsion angles are equal to 178.72(1), 170.66(5), 59.7(3), 166.76(7), 176.72(2), 152.3(1), 59.7(4) and 176.83(3)°, respectively. With an exception of Q3 (C9–N4–C10–C11 angle) and Q7 (C21–C20–C23–N6 angle) the values of angles are typical for experimentally-obtained conformations of *Imatinib* in an extended conformation (Figure 1b, [5,6]). Particularly, pyridine and pyrimidine or 4-methylphenyl and amide fragments are almost coplanar (Q1 or Q4–Q5 torsion angles are close to 180°). The Q2 = 170.66(5)° angle (N2–C9–N4–C10) between the pyridylpyrimidine and the methylbenzene moieties confirms the extended molecular conformation which was predicted to be 21.39 kJ/mol more stable than the folded one for a freebase [6].

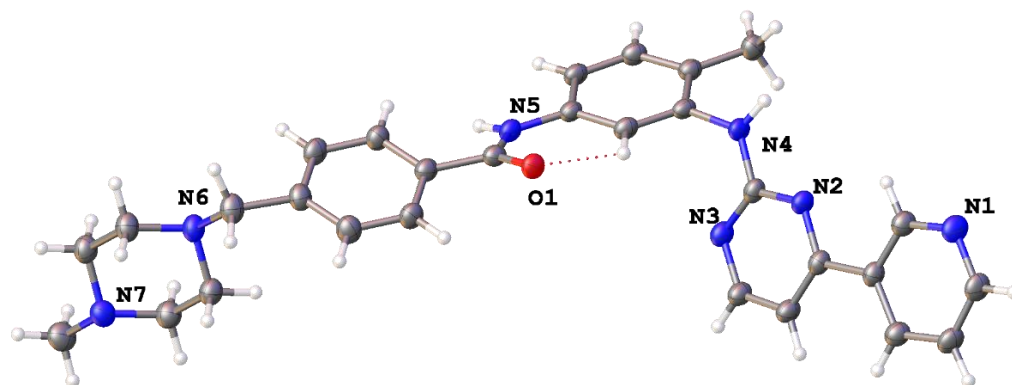


**Figure 2.** Molecular view of *Imatinib* in representation of atoms with thermal ellipsoids ( $p = 50\%$ ).

It was previously demonstrated that molecular conformation of *Imatinib* correlates well with peculiarities of its intermolecular interactions [6]. Particularly, high (up to 25%) contribution of C ... C and C ... N interactions to the Voronoi molecular surface was found to favor realization of the folded conformation. In this solid, the Voronoi molecular volume and area are equal to 646 Å<sup>3</sup> and 629 Å<sup>2</sup>, respectively, which is in accord with the average values of 677(51) Å<sup>3</sup> and 661(37) Å<sup>2</sup> previously obtained for 6 structurally characterized salts and 21 ligand–receptor *Imatinib* complexes [6]. However, despite the extended conformation, high contribution of C ... C and C ... N interactions to the molecular surface (5.5% in sum) was observed. Contribution of N ... H and O ... H

hydrogen bonds to the surface ( $80$  and  $30 \text{ \AA}^2$  as compared with previously observed  $26$ – $71$  and  $82$ – $206 \text{ \AA}^2$ ) is also unusual.

This fact can be rationalized by analysis of particular intermolecular interactions in the solid. The molecules are connected by  $\text{N-H} \dots \text{O}$  and  $\text{N-H} \dots \text{N}$  hydrogen bonds between amine and amide, and amide and pyrimidine atoms to infinite chains (Figure 3a). The values of  $r(\text{N} \dots \text{O})$  and  $r(\text{N} \dots \text{N})$  are equal to  $2.963(2)$  and  $3.167(3) \text{ \AA}$ , respectively; the  $\text{NHO}$  and  $\text{NHN}$  angles are  $166.7$  and  $166.1 \text{ \AA}$ . Note that none of these interactions are the most expected for amide and amine groups. The H-bond propensity tool [13,14] indicates that both amine and amide groups are more inclined to form hydrogen bonds with a nitrogen atom of pyridine ring [6]. Thus, one can propose that a metastable polymorph of pure *Imatinib* was obtained by us. It is also worth mentioning that the formation of two  $\text{N-H} \dots \text{N}$  hydrogen bonds also fixes carbamoylbenzyl fragments of neighboring molecules in parallel positions at  $3.3 \text{ \AA}$  which makes the formation of  $\pi \dots \pi$  interactions possible. In addition, two pyridylpyrimidine fragments also take part in stacking interactions with the interplanar distance between their parallel meanplanes as short as  $3.5 \text{ \AA}$  and the shortest interatomic distance equal to  $3.459(3) \text{ \AA}$  (Figure 3b). Thus, the significant contribution of stacking interactions to the molecular surface was observed in this solid. The strength of the pairwise interaction in staking dimer in terms of energy frameworks formalism (CrystalExplorer 17.5 program [15]) is  $-134.2 \text{ kJ/mol}$  while in dimer formed by  $\text{N-H} \dots \text{O}$  bond, the corresponding value is  $-97.2 \text{ kJ/mol}$ . In turn, the value of lattice energy is  $-489.4 \text{ kJ/mol}$ .

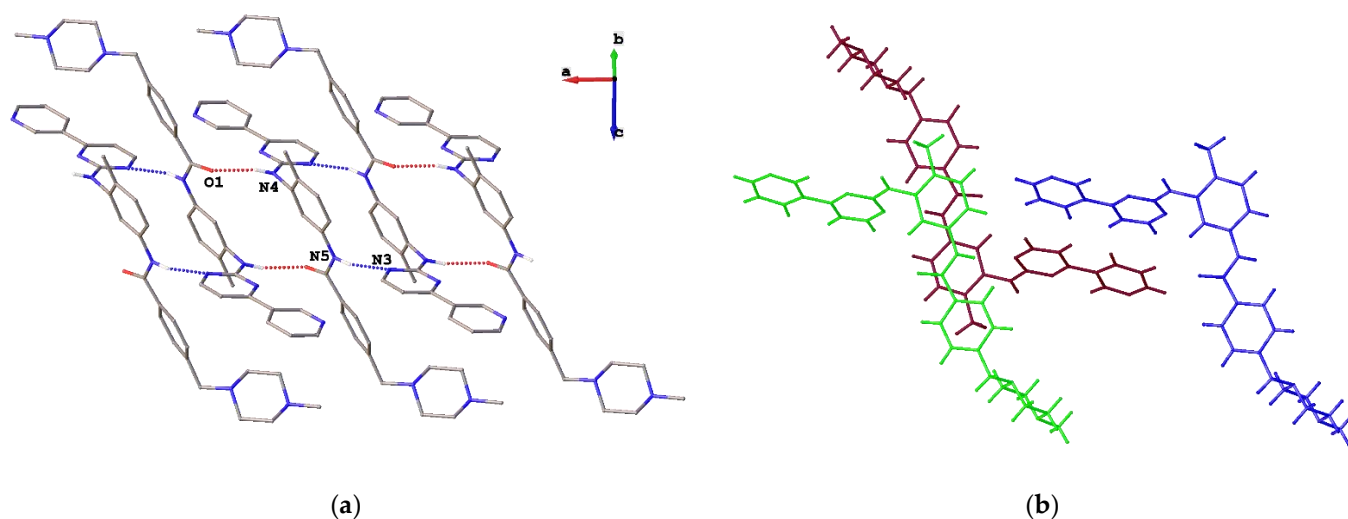


**Figure 3.** Fragment of crystal packing: (a) fragment of H-bonded chains parallel with the crystallographic a-axis; (b) stacking interactions between two pyridylpyrimidine (red and blue) and two carbamoylbenzyl (red and green) fragments.

Finally, it is worth mentioning that the observed hydrogen bonding is in accord with distribution of the molecular electrostatic potential (MEP) depicted on Figure 4. NoSphereA2 [16] instead of usual IAM refinement of X-ray diffraction data was used in order to obtain experimental MEP distribution. It allowed not only the decrease of  $R_1$  and  $wR_2$  convergence factors but also gave  $\text{H}(\text{C})$  and  $\text{H}(\text{N})$  distances ( $1.11$ – $1.16$  and  $1.02$ – $1.03 \text{ \AA}$ , respectively) close to the average values from neutron diffraction data ( $1.08$ – $1.10$  and  $1.01$ – $1.03 \text{ \AA}$ ) as obtained by Allen and Bruno [17]. The most electropositive molecular regions (shown in red) are situated in the region of the amide and amine groups. The regions of electronegative potential are situated close to the oxygen atom and near the nitrogen atom of the pyrimidine ring. Electronegative regions close to the 4-methylpiperazine are absent. This fact is in accord with theoretical calculation of low H-bond propensity of the nitrogen atom connected with the methyl group to take part in H-bonding. Experimentally-observed

H-bonding with this nitrogen in previously studied *Imatinib* salts and ligand–receptor complexes are absent as well.

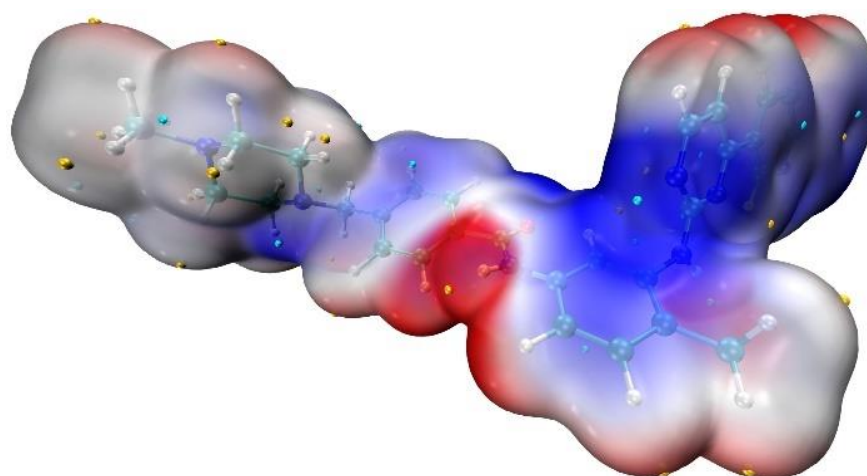


**Figure 4.** Experimental molecular electrostatic potential of free-base *Imatinib* mapped on the 0.001 a.u. isosurface of charge density ranged from  $-0.019$  a.u. (blue) to  $0.014$  a.u. (red). The negative and positive local maxima are pointed out by small blue and yellow spheres.

### 3. Materials and Methods

A solution of *Imatinib* mesylate (0.012 g, 0.05 mmol) in 1 ml of ethanol was added to a solution of arginine (0.087 g, 0.5 mmol) in 2 ml of ethanol. The mixture was heated, and the solution was cooled in air. After 2 days of standing at r.t. white precipitate formed. Single crystals of  $C_{29}H_{31}N_7O$  were obtained from this precipitate.  $T_{\text{melt}} = 484\text{--}486$  K coincides with that given in Ref. [18]. The intensities of 19559 reflections were collected at “Belok/XSA” beamline of the Kurchatov Synchrotron Radiation Source [19,20]. Diffraction patterns were collected using 1-axis MarDTB goniometer equipped with Rayonix SX165 CCD 2D positional sensitive CCD detector ( $\lambda = 0.745$  Å,  $\varphi$ -scanning in  $1.0^\circ$  steps) in the direct geometry with a detector plane perpendicular to its beam. Approximately 120 diffraction frames were collected for each data set. Thus obtained data were indexed and integrated using the XDS software suite [21]. At 100 K crystal system is triclinic, space group  $P\bar{1}$ :  $a = 8.5780(17)$ ,  $b = 10.467(2)$ ,  $c = 14.872(3)$  Å,  $\alpha = 79.78(3)$ ,  $\beta = 82.55(3)$ ,  $\gamma = 81.94(3)^\circ$ ,  $V = 1293.6(5)$  Å<sup>3</sup>,  $Z = 2$ ,  $\mu = 0.089$  mm<sup>-1</sup>,  $D_{\text{calc}} = 1.267$  g cm<sup>-3</sup>,  $F(000) = 524$ .

The structure was solved by the dual-space algorithm [22] and refined by full-matrix least squares against  $F^2$  using the NoSpherA2 algorithm [16] implemented within the Olex2 package [23]. Non-hydrogen atoms were refined in an anisotropic approximation. Hydrogen atoms were located on difference Fourier maps and included in the refinement in isotropic approximation and unfixed bond distances. Refinement converged to  $R_1 = 0.057$  (for 3907 observed reflections and 459 parameters),  $wR_2 = 0.158$  and GOF = 1.01 (for 7004 independent reflections,  $R_{\text{int}} = 0.098$ ). Crystallographic data in Crystallographic Information File (CIF) format can be downloaded online at Supplementary Materials.

Peculiarities of the Voronoi molecular polyhedra were calculated using the ToposPro package [24].

**Supplementary Materials:** Crystallographic data in Crystallographic Information File (CIF) format can be downloaded online.

**Author Contributions:** Conceptualization, A.A.K.; methodology, A.V.V.; investigation, A.V.V. and P.V.D.; writing—A.A.K. and A.V.V.; funding acquisition, A.A.K. All authors have read and agreed to the published version of the manuscript.

**Funding:** This research was funded by the Russian Science Foundation, grant number 20-13-00241.

**Institutional Review Board Statement:** Not applicable.

**Informed Consent Statement:** Not applicable.

**Data Availability Statement:** The X-ray data are available at CCDC under ref. code CCDC 2208498.

**Acknowledgments:** The authors gratefully acknowledge Changkuo Zhao (Department of Medicinal Chemistry, Zunyi Medical University) for providing spectra of freebase *Imatinib* as published in Ref. [25]. Ministry of Science and Higher Education of the Russian Federation is acknowledged for providing access to scientific literature.

**Conflicts of Interest:** The authors declare no conflict of interest.

## References

1. Carofiglio, F.; Lopalco, A.; Lopodota, A.; Cutrignelli, A.; Nicolotti, O.; Denora, N.; Stefanachi, A.; Leonetti, F. Bcr-Abl Tyrosine Kinase Inhibitors in the Treatment of Pediatric CML. *Int. J. Mol. Sci.* **2020**, *21*, 4469. [[CrossRef](#)]
2. Deininger, M.; Buchdunger, E.; Druker, B.J. The development of imatinib as a therapeutic agent for chronic myeloid leukemia. *Blood* **2005**, *105*, 2640–2653. [[CrossRef](#)] [[PubMed](#)]
3. Nagar, B.; Hantschel, O.; Young, M.A.; Scheffzek, K.; Veach, D.; Bornmann, W.; Clarkson, B.; Superti-Furga, G.; Kuriyan, J. Structural Basis for the Autoinhibition of c-Abl Tyrosine Kinase. *Cell* **2003**, *112*, 859–871. [[CrossRef](#)]
4. Schindler, T.; Bornmann, W.; Pellicena, P.; Miller, W.T.; Clarkson, B.; Kuriyan, J. Structural Mechanism for STI-571 Inhibition of Abelson Tyrosine Kinase. *Science* **2000**, *289*, 1938–1942. [[CrossRef](#)]
5. Golzarroshan, B.; Siddegowda, M.S.; Li, H.Q.; Yathirajan, H.S.; Narayana, B.; Rathore, R.S. Imatinib (Gleevec®) conformations observed in single crystals, protein–Imatinib co-crystals and molecular dynamics: Implications for drug selectivity. *J. Mol. Struct.* **2012**, *1018*, 107–112. [[CrossRef](#)]
6. Vologzhanina, A.V.; Ushakov, I.E.; Korlyukov, A.A. Intermolecular Interactions in Crystal Structures of Imatinib-Containing Compounds. *Int. J. Mol. Sci.* **2020**, *21*, 8970. [[CrossRef](#)]
7. Grillo, D.; Polla, G.; Vega, D. Conformational Polymorphism on Imatinib Mesylate: Grinding Effects. *J. Pharm. Sci.* **2012**, *101*, 541–551. [[CrossRef](#)]
8. Jasinski, J.P.; Butcher, R.J.; Hakim Al-Arique, Q.N.M.; Yathirajan, H.S.; Narayana, B. Imatinibium dipicrate. *Acta Crystallogr. Sect. E Struct. Rep. Online* **2010**, *66*, o411–o412. [[CrossRef](#)]
9. Fang, Z.-Y.; Zhang, B.-X.; Xing, W.-H.; Jia, H.-L.; Wang, X.; Gong, N.-B.; Lu, Y.; Du, G.-H. A series of stable, metastable and unstable salts of Imatinib with improved solubility. *Chin. Chem. Lett.* **2022**, *33*, 2159–2164. [[CrossRef](#)]
10. Ushakov, I.E.; Lenenko, N.D.; Goloveshkin, A.S.; Korlyukov, A.A.; Golub, A.S. Influence of noncovalent intramolecular and host–guest interactions on imatinib binding to MoS<sub>2</sub> sheets: A PXRD/DFT study. *CrystEngComm* **2022**, *24*, 639–646. [[CrossRef](#)]
11. Kabova, E.A.; Blundell, C.D.; Muryn, C.A.; Whitehead, G.F.S.; Vitorica-Yrezabal, I.J.; Ross, M.J.; Shankland, K. SDPD-SX: Combining a single crystal X-ray diffraction setup with advanced powder data structure determination for use in early stage drug discovery. *CrystEngComm* **2022**, *24*, 4337–4340. [[CrossRef](#)]
12. Goloveshkin, A.S.; Korlyukov, A.A.; Vologzhanina, A.V. Novel Polymorph of Favipiravir—An Antiviral Medication. *Pharmaceutics* **2021**, *13*, 139. [[CrossRef](#)] [[PubMed](#)]
13. Galek, P.T.A.; Allen, F.H.; Fábian, L.; Feeder, N. Knowledge-based H-bond prediction to aid experimental polymorph screening. *CrystEngComm* **2009**, *11*, 2634–2639. [[CrossRef](#)]
14. Vologzhanina, A.V. Intermolecular Interactions in Functional Crystalline Materials: From Data to Knowledge. *Crystals* **2019**, *9*, 478. [[CrossRef](#)]
15. Mackenzie, C.F.; Spackman, P.R.; Jayatilaka, D.; Spackman, M.A. CrystalExplorer model energies and energy frameworks: Extension to metal coordination compounds, organic salts, solvates and open-shell systems. *IUCr* **2017**, *4*, 575–587. [[CrossRef](#)]
16. Kleemiss, F.; Dolomanov, O.V.; Bodensteiner, M.; Peyerimhoff, N.; Midgley, L.; Bourhis, L.J.; Genoni, A.; Malaspina, L.A.; Jayatilaka, D.; Spencer, J.L.; et al. Accurate crystal structures and chemical properties from NoSpherA2. *Chem. Sci.* **2021**, *12*, 1675–1692. [[CrossRef](#)] [[PubMed](#)]
17. Allen, F.H.; Bruno, I.J. Bond lengths in organic and metal-organic compounds revisited: X–H bond lengths from neutron diffraction data. *Acta Crystallogr. B* **2010**, *66*, 380–386. [[CrossRef](#)]
18. Zimmermann, J.D. Pyrimidin Derivatives and Process for Their Preparation 1993. Patent EP0564409A1, 25 March 1993.
19. Lazarenko, V.A.; Dorovatovskii, P.V.; Zubavichus, Y.V.; Burlov, A.S.; Koshchienko, Y.V.; Vlasenko, V.G.; Khrustalev, V.N. High-Throughput Small-Molecule Crystallography at the ‘Belok’ Beamline of the Kurchatov Synchrotron Radiation Source: Transition Metal Complexes with Azomethine Ligands as a Case Study. *Crystals* **2017**, *7*, 325. [[CrossRef](#)]
20. Svetogorov, R.D.; Dorovatovskii, P.V.; Lazarenko, V.A. Belok/XSA Diffraction Beamline for Studying Crystalline Samples at Kurchatov Synchrotron Radiation Source. *Cryst. Res. Technol.* **2020**, *55*, 1900184. [[CrossRef](#)]
21. Kabsch, W. XDS. *Acta Crystallogr. D Biol. Crystallogr.* **2010**, *66*, 125–132. [[CrossRef](#)]
22. Sheldrick, G.M. SHELXT—Integrated space-group and crystal-structure determination. *Acta Crystallogr. Sect. Found. Adv.* **2015**, *71*, 3–8. [[CrossRef](#)]
23. Dolomanov, O.V.; Bourhis, L.J.; Gildea, R.J.; Howard, J.A.K.; Puschmann, H. OLEX2: A complete structure solution, refinement and analysis program. *J. Appl. Crystallogr.* **2009**, *42*, 339–341. [[CrossRef](#)]

- 
24. Blatov, V.A.; Shevchenko, A.P.; Proserpio, D.M. Applied Topological Analysis of Crystal Structures with the Program Package ToposPro. *Cryst. Growth Des.* **2014**, *14*, 3576–3586. [[CrossRef](#)]
  25. Wang, X.; Zhao, C.; Cao, Y.; Yuan, Z.; Xu, L.; Zhou, Y. Continuous flow processing: In situ preparation of imatinib freebase. *Lat. Am. J. Pharm.* **2018**, *37*, 1251–1256.